

Bolometer Results in the Long-Microwave-Heated WEGA Stellarator

D. Zhang, M. Otte, L. Giannone

*Max-Planck-Institut für Plasmaphysik, EURATOM Association, Wendelsteinstr. 1,
17491 Greifswald, Germany*

Abstract. A 12 channel bolometer camera based on a gold foil absorber has been installed on the WEGA stellarator to measure the radiation power losses of the plasma. The measured total radiation power is typically less than 30% of the ECRH input power. However, this radiated power fraction depends on the ECRH input power, the magnetic configuration and the field strength as well as the working gas. For separatrix-bounded configurations, core-peaked radiation intensity profiles are usually detected, while in a limiter-configuration they are flatter, broader and more asymmetric. In addition, significant radiation originating from the SOL region is measured for all the cases studied. The SOL radiation changes with changing the plasma-wave interaction region, indicating a strong correlation between radiation and power deposition. Under the WEGA-plasma conditions ($T_e < 10$ eV), it is considered that the radiation profile reflects the plasma pressure associated with the power deposition distribution of the ECRH.

Keywords: bolometer, Stellarator, WEGA, ECRH, radiation power loss, radiation intensity, power deposition

PACS: 52.70.-m; 07.57.Kp; 52.55.-s; 52.50.-b; 87.66.-a

1. INTRODUCTION

WEGA is a medium-size classical stellarator being operated at IPP Greifswald. The machine, which was upgraded in 2001 [1], is mainly used for educational training and testing of new diagnostic equipment and for basic research in plasma physics [2]. The plasma is heated by an ECR at 2.45 GHz and reaches a typical electron temperature of several electron volts. Two launching antennas at different toroidal positions are available and yield, respectively, a maximum heating power of 6 and 20 kW. The heating scenario is characterized by the long wave length (about 12 cm), which is comparable with the plasma radius of WEGA (~ 10 cm). In this case, the heating efficiency is highly sensitive to the power deposition profile which, for a given launching angle and a working mode of the ECRH, depends strongly on the magnetic configurations and the background plasmas. In the low T_e -range (< 10 eV), the radiation loss function of the working gases increases monotonously with increasing T_e [3, 4]. Therefore, in the case of a rather low impurity concentration in WEGA as indicated by spectroscopic measurements, the angular radiation profile measured by the bolometer reflects the plasma pressure profile which is strongly associated with the power deposition distribution of the ECRH. In this sense, the bolometer camera on WEGA can be used to monitor the optimization process of the ECR-absorption and of the plasma energy content. On the other hand, the bolometry on WEGA serves for testing the critical technical aspects of a bolometer under steady state operation as planned for W7-X [5]. The main issues for steady state operation are the thermal drift and real-time data storage and processing.

2. DIAGNOSTIC SET-UP

The bolometer is of a miniaturized metal foil type, used in several fusion machines such as ASDEX Upgrade, W7-AS, LHD and JET [6]. A $4 \mu\text{m}$ thick gold foil, deposited on a $7.5 \mu\text{m}$ Kapton foil substrate, is chosen as an absorber. It is sensitive to the incident energy in the range from 2.5 eV to 7 keV with absorption coefficients above 85% [7].

The 12 channel bolometer array is positioned on the mid-plane, viewing the plasma from the low-field side. A slit with a dimension of $0.5\text{cm}\times 2.0\text{cm}$ is used as an aperture, providing a poloidal spatial resolution of 6 cm. The length of the slit (2.0 cm) is necessary for obtaining enough signal-to-noise ratio. The viewing window is opened poloidally to $\pm 47^\circ$ and covers the whole cross-section, as shown in Fig.1.

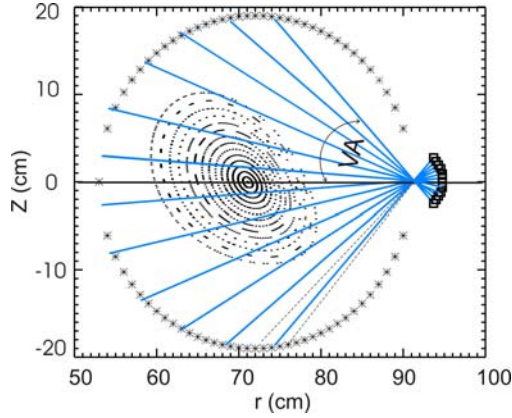


FIGURE 1. Location and lines of sight of the 12 channel bolometer array. Region between the two dashed lines corresponding to the viewing window of the channel with a viewing angle (VA) of -47° .

The bolometers are excited by a 19.2 kHz and 20 V sine-wave driver signal. The offset of the electronic system are minimized automatically before each discharge. The raw signals are firstly amplified with a gain of 1804 before transferred into an ADC card. Data acquisition with a sampling rate of 2.5 kHz is used. The optimal temporal resolution is 1 ms. Using LabView 6.1, the measurements can be controlled through remote operation. An in-situ calibration [8] is performed automatically after each measurement, providing the required parameters for further data processing. A sensitivity of about $200 \mu\text{W}/\text{cm}^2$ has been realized.

Angular profiles of radiation intensity are derived from the measured line-integrated signals by taking the optical geometry into account. The total radiation loss is simply obtained by linear extrapolating the calculated power in the viewing range to the whole torus volume.

3. MEASUREMENT RESULTS

Up to now, three types of ECRH antenna have been tested in order to optimize the heating efficiency. They are wave-guides of 90° -cutting, 45° -cutting and of a two-slot type. Peaked density profiles and relatively-high plasma densities and temperatures are only achieved with the two-slot antenna. The results presented below were obtained for the two-slot antenna heated plasmas. For these plasmas there exist well documented measurements with the Langmuir probe [9].

3.1 Dependence of Radiation Level on B-field Strength

First, it is observed that the total radiation power depends strongly on the magnetic field strength. Fig. 2 shows the level of the total radiation from Ar-plasmas as a function of the axis field strength B normalized to B_0 , with $B_0=87.5$ mT being the field strength resonant to the ECRH. The total radiation from the bolometer shows a maximum at $B/B_0\sim 0.60$. It is interesting to note that the highest plasma temperature and line-averaged density have been observed by the Langmuir probe and interferometer [9] in the range of B/B_0 from 0.60 to 0.65. The correlation between the plasma pressure and the bolometer signal can be understood as, in the low T_e -range ($<10\text{eV}$), both increasing the plasma density and temperature will lead to an increase in radiation intensity of the plasma. The improved energy content is suggested to be a result of an increased ECR-heating efficiency associated with a possible O-X-B mode conversion [10].

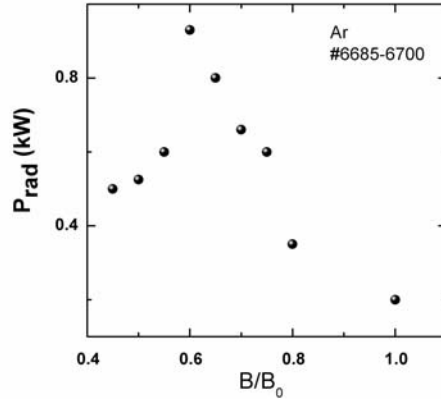


FIGURE 2. Dependence of the radiation power loss on the normalized B-field strength for separatrix Ar-plasmas with an ECRH input power of 6 kW.

3.2 Dependence of Radiation Distribution on Configuration

The angular distribution of the radiation intensity depends strongly on the shape of the magnetic flux surface and the position of the magnetic axis. Fig. 3 (left) compares the line-averaged radiation intensity profiles of Ar-plasmas between two configurations with $\iota_0/2\pi=0.2$ and 0.44 . In the $\iota_0/2\pi=0.2$ configuration, smooth magnetic flux surfaces are cut by the ECR-antenna, whereas, in the higher- ι_0 case, the plasma is limited by a separatrix. A core-peaked radiation profile is observed for the separatrix-bounded configuration and the radiation peak in the core vanishes in the limiter configuration with $\iota_0/2\pi=0.2$. In both cases, the angular radiation profiles are up/down-asymmetric and this asymmetry becomes more pronounced in the limiter case.

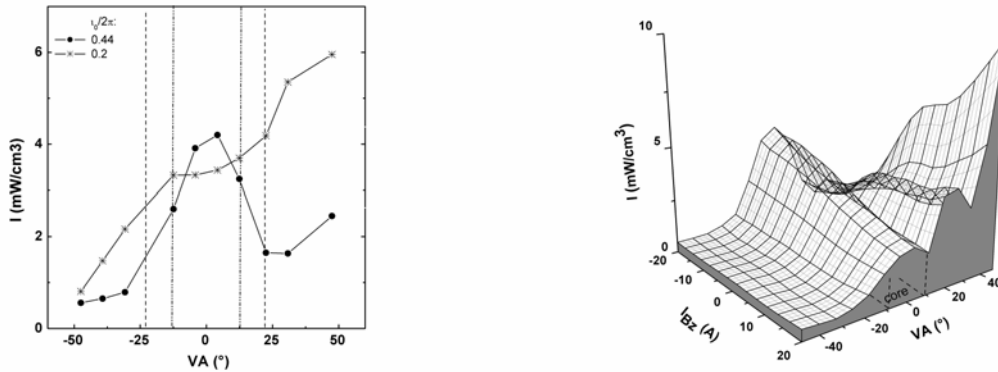


FIGURE 3. (Left) Comparison between the angular profiles of the line averaged radiation intensity of separatrix- and limiter-plasma. Regions inside the two dotted and point-point-dotted lines corresponding to the viewing windows of the bolometers to the core plasma with $\iota_0/2\pi=0.2$ and 0.44 , respectively. (Right) Dependence of the radiation intensity profiles on the applied vertical magnetic field B_z , with I_{Bz} standing for the used current. The viewing window of the bolometers to the core plasma is marked with dotted lines.

The situation becomes more complex when a vertical B-field is applied to shift a separatrix-configuration horizontally with respect to the ECR-antenna, as shown in Fig. 3 (right). When gradually shifting the plasma towards the antenna by increasing I_{Bz} , the peak in the center is reduced and new peaks appear in the SOL region, with the maximum radiation shifting to or even beyond the upper boundary of the view-window of the bolometer. This multi-peaked radiation picture is repeatable and robust in the sense that it is seen for $\iota_0/2\pi=0.44$ and 0.56 configurations and in H_2 -, He- and Ar-plasmas. It is worth noting that the peaked radiation in the upper SOL region of Ar-plasmas can be reduced by shaping the magnetic configuration facing the launching antenna through changing the polarity of the helical current or by using another antenna, which lies at a different toroidal position. All these phenomena above indicate that the power deposition is sensitive to the plasma-wave interaction region.

3.3 Dependence of the Global Radiation Level on the ECRH-power

Generally, the total radiation power loss P_{rad} increases with increasing the ECRH-heating power P_{ecrh} , while the radiation profile for a given configuration remains more or less unchanged, as shown in Fig. 4 (left). However, the radiated power fraction, i.e. the ratio of P_{rad} to P_{ecrh} , decreases. This is true for all the three investigated working gases, which is presented in Fig. 4 (right). The typical value of $P_{\text{rad}}/P_{\text{ecrh}}$ is less than 30%. It is also found that the radiation loss for limiter plasmas is larger than for separatrix-bounded plasmas [2].

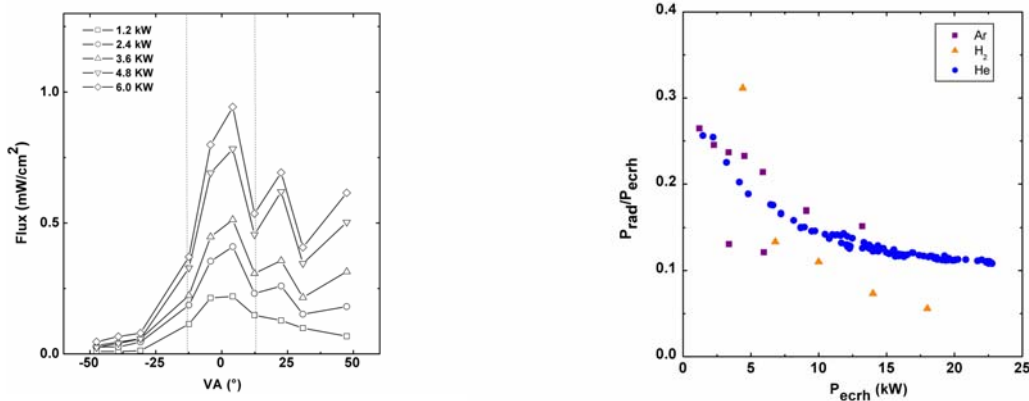


FIGURE 4. (Left) Radiation power flux distributions for Ar-discharges ($u_0/2\pi=0.56$) with different ECRH input powers. (Right) Dependence of the total radiated power fraction $P_{\text{rad}}/P_{\text{ecrh}}$ on the ECRH input power for separatrix Ar- H₂- and He-plasma.

4. DISCUSSION

Since the Au foil bolometer is also sensitive to the thermal energy of the incident neutral particles, the bolometer results shown throughout this paper may not be due only to radiation. The contribution from the neutral particle flux will be estimated later by using additional silicon photodiode arrays. On the other hand, the lower sensitivity of the Au absorber for the radiation energy below 2.5 eV does not play a crucial role here because expanding the absorption response window through blackening the detector surfaces with C-coating did not lead to a remarkable increase of the bolometer signal strength for H₂-discharges. A significant improvement of absorptivity in low energy range, whereas, has been clearly demonstrated in laboratory using different laser as light sources. Such tests will be extended to Ar- and He-discharges.

ACKNOWLEDGMENTS

The authors gratefully acknowledge the design of the bolometer camera made by A. Fohr and the technical supports provided by D. Aßmus and N. Paschkowski.

REFERENCES

1. J. Lingertat et al., 30 EPS Conference on Plasma Phys. and Contr. Fusion, St. Petersburg, 7-11 July 2003, P-1.10 (2003).
2. M. Otte et al., 31 EPS Conference on Plasma Phys. and Contr. Fusion, London, July 2004, P-1.211 (2004).
3. D.E. Post et al., Atomic Data and Nuclear Data Tables **20**, 397-439 (1977).
4. P.C. Stangeby, *The Plasma Boundary of Magnetic Fusion Devices*, Bristol: Institute of Physics Publ.(IoP), 2000, pp. 130-145.
5. H.J. Hartfuss et al., Review of Scientific Instruments **68**, 1244 (1997).
6. K.F. Mast et al., Review of Scientific Instruments **62**, 744 (1991).
7. http://www-cxro.lbl.gov/optical_constants/index.html
8. L. Giannone et al., Review of Scientific Instruments **73**, 3205 (2002).
9. K. Horvath, "Characterisation and Optimisation of WEGA Plasmas", Ph.D. Thesis, Greifswald University, 2005.
10. H. P. Laqua et al., Physical Review Letters **78** (18), 3467-3470 (1997).